Study of Optical Property of Ce^{3+} doped $Li_{15}(SO_4)_5F_4Cl$ Unique Halosulphate Phosphor

A. M. Bhake

Department of Physics, Gondwana University, Gadchiroli- 442605, India.

aparna.dhond@gmail.com

Abstract

For the first time in phosphor history, a remarkable series of Ce^{3+} ion-doped Lithium Fluoride Chloride Sulphate i.e., $Li_{15}(SO_4)_5F_4Cl$ alkaline halo sulphate phosphors are made using a wet chemical process. Using X-ray diffraction (XRD) tests, the phase creation and concentration were ascertained. Additionally, Fourier Transform Infrared (FTIR) spectroscopy was used which makes it possible to identify the chemical linkages successfully and browsing electron microscopy was tested for surface investigations (SEM). When the photoluminescence (PL) characteristics of the as-prepared phosphors were examined, it was discovered that the Ce^{3+} ions in these hosts produced a broad Ultra-Violet (UV) emission. These could be used for scintillation and as potential UV lamp phosphors.

Keywords: Halo Sulphates, Phosphor, Wet Chemical Method, Ce^{3+} ions, Photoluminescence, UV.
Received 29 January 2025; First Review 11 March 2025; Accepted 19 March 2025.

*** Address of correspondence**
A. M. Bhake
Department of Physics, Gondwana University, Gadchiroli- 442605, India

Email: aparna.dhond@gmail.com

How to cite this article
A. M. Bhake, Study of Optical Property of Ce^{3+} doped $Li_{15}(SO_4)_5F_4Cl$ Unique Halosulphate Phosphor, J. Cond. Matt. 2025; 03 (01): 91-95.

Available from:
https://doi.org/10.61343/jcm.v3i01.88

Introduction

Brilliant materials (phosphors) doped with rare earth particles assume a crucial part in current life, because of their phenomenal applications going from fluorescent lights, scintillators, variety shows, heightening screens, ionizing radiations dosimetry, etc. [1-3]. The electric and photosensitive characteristics of phosphors are significantly impacted by the substance structure, degree of underlying issue, abandonments, and the existence of dopants or debasements. Lately, there has been a lot of attention in the glowing qualities of Ce^{3+} doped structures [4-6]. Tinny film electroluminescence displays, imaging plates, luster, solid-state illumination, and thermoluminescence dosimetry are among the promising applications for the alkaline halosulphates produced with Ce^{3+} particles [7-9]. Because of its simplicity of readiness and phenomenal photoluminescence and thermoluminescence qualities, a few examinations on chloride-based halosulphate materials are likewise in the works, as countless halosulphate materials have a few fascinating optical properties [7, 10]. Because of their numerous uses, chloride-based materials have witnessed a steady increase in interest in the last two-three years. By studying optical retention, electron spin impact, photonic movement, several kinds of refractive indices, and other real features like versatile modulus, a few organizations have made significant attempts to focus on the deformities in these materials [11-14]. Ce^{3+} is an exclusive activator for scintillator applications due to its extremely fast and efficient transition as well as energy close to the sensitivity maximum of photomultiplier tubes [15, 16]. Among the uses for inorganic scintillators are dental and medical diagnostic applications. High-energy radiation detection and visualization have been made possible in large part by these mineral scintillators. The most usually employed scintillators at the moment are bismuth germanate, cesium iodide and sodium iodide fixed with thallium [17]. These have a good energy resolution, high density light production and a comparatively rapid fade time. With remarkably short decay durations of just 0.8 and 4.4 ns, BaF_2 and CsF_2 are utilized for applications that demand fast response. Their light production is relatively modest, nevertheless. There is still a great need for scintillators with better features for certain uses, and there is currently no scintillator that combines a high light yield with quick response. Since halosulphates are thought to meet these requirements, more effort is being put into creating novel materials with higher efficiency. In light of this, numerous analyses of the iridescence of Ce^{3+} in halosulphate phosphors were conducted [18]. Cerium-activated phosphors are typically regarded as expanding groups and transmit in the ultraviolet or spectral region. In any case, the Ce^{3+}-discharge is shifted to longer frequencies by the host cross section's crystal field. Because it can efficiently emit light when excited, usually in the ultraviolet (UV) or bluish range, the Ce^{+3} ion is used in this situation.

It is a useful part of specialist phototherapy equipment because of its luminous qualities [19].

In this paper, the iridescence property of Ce^{3+} particles actuated $Li_{15}(SO_4)_5F_4Cl$ halosulphate phosphors arranged by wet chemical method is being accounted for first time throughout the entire existence of phosphors.

Method

The wet chemical strategy is used to set up the series of Ce^{3+} doped $Li_{15}(SO_4)_5F_4Cl$ halosulphate phosphors. This is by far the simplest and best incorporation method when compared to the many different usual techniques [20]. Using a logical equilibrium of precision 0.0001gm, the precursors of AR grade with the highest virtue (99.99% pure) $Li_2(SO_4)$, LiCl, NH_4F, and $Ce_2(SO_4)_3$ were demonstrated up stochiometric proportion. The natural substances were broken down in twofold refined de-ionized water in an exceptionally dry climate and later, every one of the arrangements of the forerunners were merged individually. The resultant arrangement was saved for amalgamation on magnetic stirrer for 30 min. The series of Ce^{3+} doped phosphors were ready according to the various fixations going from 0.1, 0.5, 1, 2, 5, and 10 mol% in the host framework. The straightforward arrangement acquired was saved for drying in a stove for 24 hours at 80 °C. The mixture turned into a smooth white powder. It was then ground into a fine powder using a stone crusher and grinder to get it ready for a number of experiments, including electron microscopy, phosphorescence, X-ray imaging, Fourier transform spectral analysis, and more [20].

A PAN data-driven diffractometer (Cu-Kα radiation) with a miniflex 2 goniometer was implemented to test the phase perfection and crystallinity of the pre-arranged $Li_{15}(SO_4)_5F_4Cl$ phosphor using X-beam deflection test in the acute angle 2θ region with a continuous examination step of 0.011 degrees and a continuation season of 15-20 seconds. Then, at that point, for testing their optical property, the above said series of phosphors was tried for photoluminescence (PL) investigation.

Operating a 150Watt 'Xenon band illumination ' as a stimuli source and a sensitive photomultiplier tube, theRF-5301PC spectrofluoro-photometer completed the PL estimates. Using a high sensitivity spectral slit width of less than 2 nm, excitation and discharge spectra were acquired.

This spectrophotometer gives revised excitation and emanation spectra in the frequency scope of 220-400 nm and 300-700 nm separately.

Checking electron microscopy (SEM) for surface morphology and Fourier change infrared (FT-IR) spectroscopy for the distinguishing proof of chemical bonds were additionally done for the previously mentioned radiance sulphates [20].

In addition to the above material, a similar method of synthesis was being adopted here for the phosphor $Li_{15-x}R_x(SO_4)_5F_4Cl$: Ce^{3+} (R = Na, K) with only the difference of precursor of dopant/co-dopant and its concentration values in mol%.

Discussion

XRD pattern of pure Li15(SO4)5F4Cl phosphor

Fig. 1 shows the XRD pattern for lithium fluoride chloride sulphate phosphor. Accordingly, there is no standard JCPDS document to coordinate with the XRD.

Example of this phosphor thus it's exceptional because for the first time in phosphor history, it is prepared and tested.

The fact that the material was translucent makes it seen with highly intense sharp peaks. It typically indicates the presence of well-ordered repeating crystalline structure.

The interatomic spacing within the crystal lattice is dependent on peak position. Changes in peak positions can indicate variations in lattice parameters due to strain, impurities, or phase transitions.

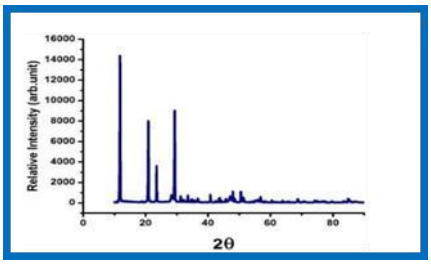

Figure 1: XRD pattern of pure $Li_{15}(SO_4)_5F_4Cl$ host material.

FT–IR study of Ce^{+3} doped Lithium fluoride chloride sulphate phosphor

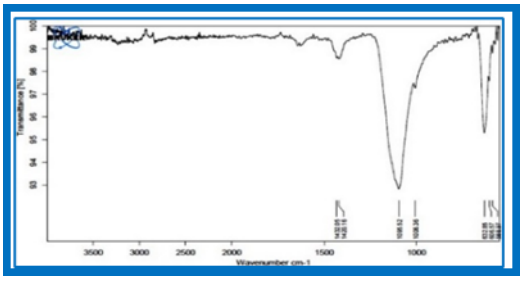

Figure 2: FT-IR ranges of Ce^{+3} doped Lithium fluoride chloride sulphate phosphor.

An IR spectrum of a chemical substance is a unique fingerprint for its identification about chemical bonds and material composition. It provides useful information about the structure of molecules quickly. FT-IR fields of $Li_{15}(SO_4)_5F_4Cl$:Ce^{3+} phosphor as shown in Fig. 2. Two

strong and extensive bands: one is due to $Li_2(SO_4)$ at 1095 cm^{-1} and another band is due to cerium at 632 cm^{-1}. Weak bands near 1432 cm^{-1} may be due to ammonium fluoride were displayed for the phosphor.

SEM analysis of $Li_{15}(SO_4)_5F_4Cl:Ce^{3+}$ phosphor

The $Li_{15}(SO_4)_5F_4Cl$ phosphor's crystallite size is visible in the SEM micrograph, which shows highly detailed magnified image as shown in Fig. 3a, 3b, 3c. Typically, crystallites are between two to five micrometres in size.

The crystallites have a crisp surface shape. The particles are composed of lengthy structure, it means tend to cluster together, forming larger structures. Fig 3 (a). Also, it shows remarkably agglomerated crystallites and have a strongly constructed particles appear robust and well-formed. Its layers-like appearance shows the structure seems to have multiple layers, possibly resembling a sheet-like or stacked formation Fig. 3 (b), 3 (c).

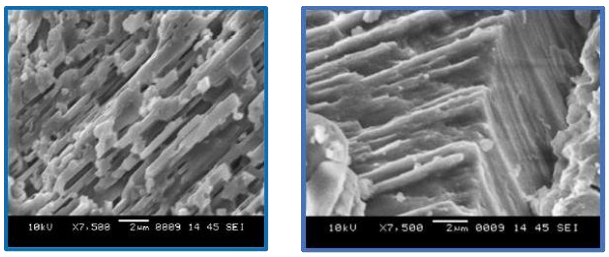

(a) (b)

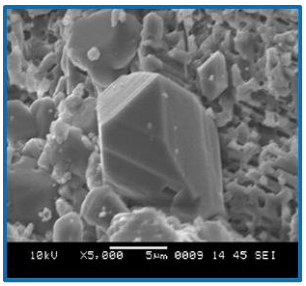

(c)

Figure 3 (a), (b), and (c): Surface Morphology of $Li_{15}(SO_4)_5F_4Cl$ phosphor

Photoluminescence (PL) in Ce^{3+} doped $Li_{15}(SO_4)_5F_4Cl$ Phosphor

In the Ce^{3+} doped lithium fluoride chloride sulphate host lattice, the PL excitation spectrum of Ce^{3+} ions reveals wideband fluorescence with a highest intensity at 254 nm and an inclined peaking at 236 nm when stimulated at 340 nm. Fig. 4 illustrates an electron from the $4f^1$ orbital is moved to the $5d^1$ orbital when Ce^{3+} absorbs energy. Due to its stronger interactions with the surrounding ions and greater spatial extension, the $5d^1$ orbital undergoes considerable crystal potential splitting.

The wavelengths of emission of lithium fluoride chloride sulphate phosphors series at various doping ratios are presented in Figs. 5(i) and 5(ii) when exposed at 254 nm of wavelength. When activated by 254 nm UV light, the phosphors show broadband emission that stretches from 260 to 406 nm with a maximum of roughly 325 nm. Other than intensity variations, the phosphors remain unchanged with changing dopant concentrations. Because of the splitting of its 4f ground state, Ce^{3+} emission should consist of a double band. However, in this instance, it is not possible to immediately discern between the emission spectrum's doublet bands.

Consequently, it splitted into two separate Gaussian components, as shown in Fig. 6(iii), with peak centres on the energy scale at 31152.64 cm^{-1}(321 nm) and 28248cm^{-1} (354 nm). The energy difference between these two bands is 2904 cm^{-1}. The Stoke's shift is found to be 8600 cm^{-1}. The shift in PL intensity of Lithium fluoride chloride sulphate phosphors with Ce^{3+}- doping level is depicted in Fig. 6(i). It is discovered that as the doping concentration rises, the emission intensity of the Ce^{3+} ions first increase before peaking at x = 0.01. The concentration quenching effect then causes the intensity to drop as the concentration rises further [21]. When the dopant concentration is sufficiently high, the following equation connects the luminous intensity I to the dopant concentration x,

$$\frac{I}{x} = k\,[1 + \beta.x^3]^{\theta-1} \qquad (1)$$

This equation can be loosely written as follows for a specific host matrix as

$$log\frac{I}{x} = c - \frac{\theta}{3}\log x \qquad (2)$$

where k, β, and c are constants for the same excitation state [21].

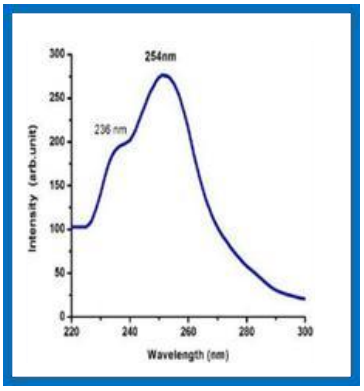

Figure 4: Pattern of Ce^{3+} doped $Li_{15}(SO_4)_5F_4Cl$ phosphor excitation

The electric multipole index, θ, illustrates collaborations between electric dipoles, dipoles-quadrupoles and electric quadrupoles when its values are 6, 8, and 10. Fig. 6(ii) shows the association between log (I/x) and log (x) for

lithium fluoride chloride sulphate (x > 0.01) phosphor based on its emission spectra acquired at 325 nm. The plotted data's gradient, $(-\theta/3)$ = -3.3859, was found to be appropriate for a straight line. As a result, θ is 10.1577, which is rather near to 10. In addition to making the materials stable and potentially useful for high-resolution displays, electroluminescent devices, vacuum discharge lamp phosphor screens, etc., This implies that the concentration quenching of Ce^{3+} luminous intensity is mostly caused by the electric quadrupole–electric quadrupole interaction mechanism.

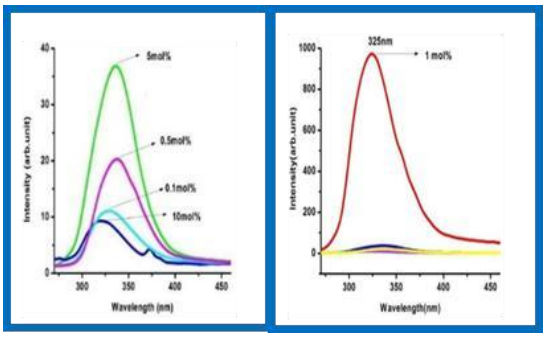

Figure 5: (i) $Li_{15}(SO_4)_5F_4Cl:Ce^{3+}$ phosphor emission spectrum, with the exception of 1 mol%. **(ii)** $Li_{15}(SO_4)_5F_4Cl:Ce^{3+}$ emission spectrum at 1 mol%.

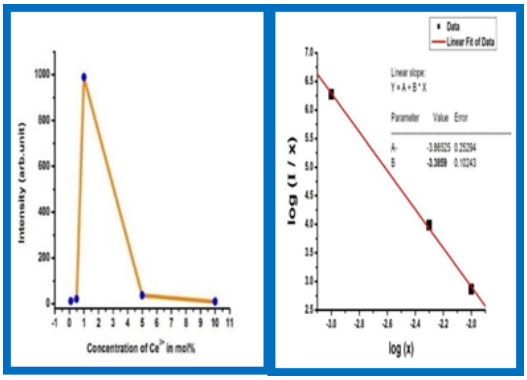

Figure 6: (i) The PL influence verses doping concentration in mol%, **(ii)** The plot of log(I/x) versus log(x) for $Li_{15}(SO_4)_5F_4Cl:Ce^{3+}$phosphors is linear.

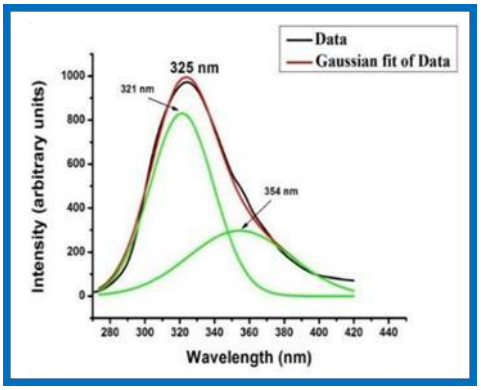

Figure 6 (iii): Gaussian functions (λ_{exc} = 254 nm) were used to fit the PL spectra of $Li_{15}(SO_4)_5F_4Cl:Ce^{3+}$ phosphors, which has an emission peak at 325 nm.

Photoluminescence in Ce^{3+} doped $Li_{15-x}Na_x(SO_4)_5F_4Cl$ Phosphor

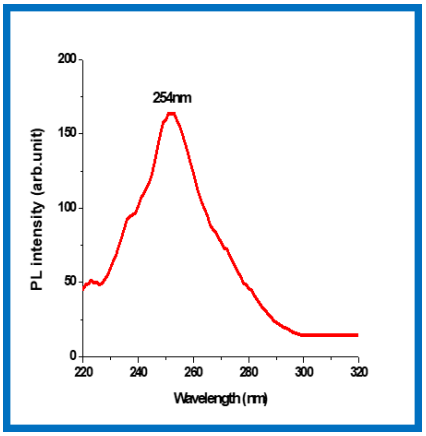

Figure 7: Excitation spectra of $Li_{15-x}Na_x(SO_4)_5F_4Cl:Ce^{3+}$ 1 mol% (R=Na, K) as x= 1, 3, 5, 10 mol%.

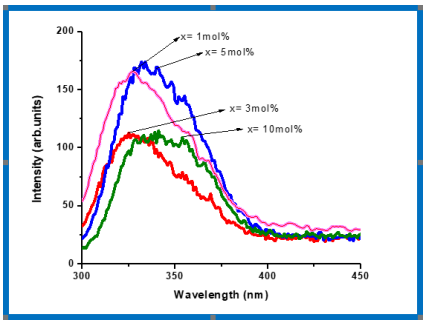

Figure 8: Emission patterns of $Li_{15-x}Na_x(SO_4)_5F_4Cl:Ce^{3+}$ 1 mol%.

An attempt is made to study the $Li_{15}(SO_4)_5F_4Cl$: Ce^{3+} phosphor by co-doping it with sodium (Na^+) ions in the host crystal lattice. It is monitored that in the case of $Li_{15}(SO_4)_5F_4Cl$: Ce^{3+} phosphor, the PL intensity was exceptional for 1 mol% of Ce^{3+} [Fig. 5 b]. For $Li_{15-x}Na_x(SO_4)_5F_4Cl:Ce$:1 mol%, Fig. 7 and 8 display the excitation and emission spectra, respectively for x = 1, 3, 5, 10 mol% of sodium (Na^+) ions. In this case, the prominent excitation is peaking at 254 nm which overlaps very well with Hg emission (253.7 nm) and we obtained the broadband emission at around 327 nm for different concentrations of Na^+ as x =1, 3, 5, and 10 mol%. It is evident from Fig. 8 that the PL intensity is lowest at 10 mol% of Na^+ ions and highest at 5 mol%. Co-doping Na+ ions in the host matrix is thought to cause concentration quenching, which significantly reduces the total PL intensity. On the other hand, weak spin-orbit coupling of the ground state of Ce^{3+} ions are indicated by the single peaking at about 327 nm [22].

Photoluminescence in Ce^{3+} doped $Li_{15-x}K_x(SO_4)_5F_4Cl$ Phosphor

Similarly by keeping Ce^{3+} constant at 1 mol%, the new host $Li_{15-x}K_x(SO_4)_5F_4Cl$: Ce^{3+} 1 mol% phosphor was synthesized

by the wet chemical method in which lithium-ion is being replaced by potassium ion. Figure 7 and Figure 9 display the excitation and emission pattern of $Li_{15-x}K_x(SO_4)_5F_4Cl$: Ce^{3+}:1 mol%, respectively for x = 1, 3, 5, 10 mol% of potassium (K^+) particles. The excitation spectra have prominent maxima at 254 nm which well matched with Hg emission (253.7 nm) and monitored the broadband emission at around 325 nm-355 nm for different concentrations of K+ as x =1, 3, 5, and 10 mol%. From Fig. 9, The PL intensity is seen to be lowest at 3 mol% of K^+ ions and highest at 1 mol%. Once more, it is claimed that co-doping K^+ ions in the host matrix causes concentration quenching, which significantly reduces the overall PL intensity. On the other hand, the single peaking at about 325–355 nm suggests that the ground state of Ce^{3+} ions have a modest spin-orbit/loop coupling. The strong crystal field at the Ce^{3+}site, which predominates over the spin-orbit/loop coupling, could be the cause of the minor shift towards a longer wavelength [22].

However, the fact that the PL emission intensity is higher (Fig. 9, 700 A.U.) when K^+ ions are doped in the host matrix as opposed to when Na^+ ions are doped (Fig. 8, 175 A.U.) suggests that K^+ ions are predominating in the replacement of lithium ions.

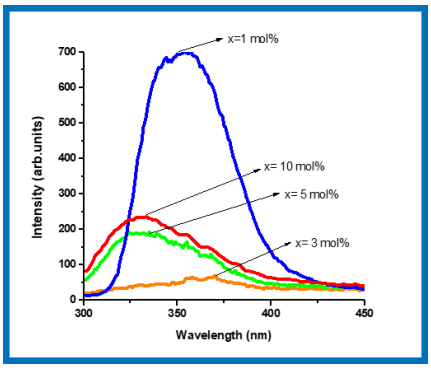

Figure 9: Shows the host $Li_{15-x}K_x(SO_4)_5F_4Cl$: Ce^{3+}:1 mol% emission pattern.

Conclusion and Future Prospective

The luminous characteristics of $Li_{15}(SO_4)_5F_4Cl$ halosulphate phosphor doped with polycrystalline Ce^{3+} ions were successfully synthesized using wet chemical synthesis and are being reported for the first time in phosphor history. These phosphors' morphological, spectroscopic, and structural characteristics were examined using SEM, FTIR and XRD, respectively. The PL emission spectra of the three phosphors listed above were all found to be in the near-UV range. When exposed to 254 nm UV illumination, a 1 mol% concentration of $Li_{15}(SO_4)_5F_4Cl$: Ce^{3+} phosphor showed a remarkable PL emission intensity at 325 nm wavelength.

Because of their effective broad-band emission in the ultraviolet spectrum, all of the Ce^{3+} doped phosphors discussed in this paper may find use in scintillation applications. These phosphors' optical features suggest that they could be useful materials for luminous phosphors in the ultraviolet (UV) band, which spans from 300 nm to 450 nm and be used for glimmer. A thorough examination of these phosphors' additional features will undoubtedly demonstrate their merit for a wide range of future uses.

References

1. M. Mohapatra, B. Rajeswari, N. S. Hon, R. M. Kadam, V. Natarajan, J. Lumin., 166: 1, 2015.
2. A. Pandey, V. K. Sharma, D. Mohan, R. K. Kale, P. D. Sahare, J. Phys. D: Appl. Phys. 35: 1330, 2002.
3. G. N. Nikhare, S. C. Gedam, S. J. Dhoble, Lumin. 30: 163, 2015.
4. V. C. Kongre, S. C. Gedam, S. J. Dhoble, Luminescence, 2015. DOI 10.1002/bio.2875.
5. A. Poddar, S. C. Gedam, S. J. Dhoble, Luminescence, 2014. DOI 10.1002/bio.2755.
6. B. P. Kore, N. S. Dhoble, S. P. Lochab, S. J. Dhoble, J. Lumin. 145: 299, 2014.
7. E. V. D. van Loef1, P. Dorenbos1, C. W. E. van Eijk1, K. W. Kramer, and H. U. Gudel Phys. Rev. B 68: 045108, 2003.
8. V. C. Kongre, S. C. Gedam, S. J. Dhoble, J. Lumin. 135:55, 2013.
9. A. Poddar, S. C. Gedam, S. J. Dhoble, J. Lumin. 149:245, 2014.
10. S. C. Gedam, S. J. Dhoble, J. Lumin. 142:139, 2013.
11. H. Meeks, A. Janner, Phys Rev B. 38 :8075, 1988.
12. G. Wahlstrom, K. Chao, Phys Rev B. 36: 9573, 1987.
13. S. Y. Jeong, M. S. Jang, S. K. Han, S. Haussuhl, Cryst Res Tech. 27:883,1992.
14. K. Annapurna, R. N. Dwivedi, S. Buddhudu, Mater Lett. 53: 359, 2002.
15. K. W. Kramer, P. Dorenbos, H. U. Gudela and C. W. E. van Eijk, J. Mater. Chem. 16: 2773, 2006.
16. Growth and Evaluation of Improved CsI:Tl and NaI:Tl Scintillators. Crystals 12: 151,2022. https://doi.org/10.3390/cryst12111517.
17. P. Dorenbos, J. Lumin. 91: 155, 2000.
18. S. C. Gedam, S. J. Dhoble, S. V. Moharil, J. Lumin. 126 :121, 2007.
19. G. B. Nair, S. J. Dhoble, Luminescence, 2015. DOI 10.1002/Bio.2919.
20. A. M. Bhake, G. Nair, G. D. Zade, S. J. Dhoble, J. BC Lumin., 2016. DOI 10.1002/bio.3131.
21. Sandra Barysaite, Jevgenij Chmeliov, Leonas Valkunas, and Andrius Gelzinis*Cite This: J. Phys. Chem. B, 128: 4887−4897, 2024.
22. A. Nag. T. R. N. Kutty, Mat. Che. and Phy., 91: 524-531, 2005.